Method for nanostructuring of Ag atoms on Ni(111) surfaces

S. Nakanishi and K. Umezawa
Department of Physics, Osaka Prefecture University, Sakai 599-8531, Japan

M. Yoshimura and K. Ueda
Toyota Technological Institute, Hisakata, Tenpaku-ku, Nagoya 468, Japan

(Received 22 June 2000)

The nanostructuring process of Ag atoms on the Ni(111) surface was investigated in two different ways: (1) the use of a morphological change caused by Pb deposition onto the Ag-covered Ni(111) surface and (2) the use of Volmer-Weber growth mode by Ag depositions onto the Pb-covered Ni(111) surface. In case (1), the preexisting Ag layer was transformed into three-dimensional islands (nanocrystals) during Pb deposition at room temperature: The nanocrystals were directly on the Ni(111) surface and surrounded by a monoatomic Pb layer. In case (2), the Ag nanoparticles were formed not on the bare Ni(111) surface, but on the preexisting Pb layer: The particles were found to be mobile under the interaction with scanning tunneling microscopy tip. The results were discussed in terms of simple thermodynamic considerations and growth kinetics.

I. INTRODUCTION

Growth morphologies of surfaces in the metal/metal epitaxy systems are influenced roughly by the thermodynamic properties of the deposited materials and the substrate when deposition proceeds under appropriate condition of deposition rates and temperatures to achieve thermal equilibrium, although kinetic properties, the diffusion length, and the mobility of the adatoms, are also important for the smoothness of the growing film or island shapes and densities, if the island growth is the case. Surfactant-mediated epitaxy[1–5] is one of the attractive methods for manipulating the growth morphology from the Volmer-Weber [three-dimensional (3D) island growth] to the Franck–van der Merwe growth (layer-by-layer growth) and frequently studied in order to obtain well-defined crystal properties of deposited thin films. In this case, the surfactant acts to reduce surface-free energy of the system by covering the growth front incessantly without incorporating on top of the growing film.[5] On the one hand, the 3D island growth is also important for the recent development of nanostructuring technologies. According to the classical criterion for film growth,[6] 3D island growth (the Volmer-Weber mode) is expected to proceed when a metal with greater surface energy is deposited onto a metal substrate with much lower surface energy. The 3D growth is often observed as a formation of nanometer size particles depending on the diffusion length and mobility of adatoms. In the case of coadsorption of two kinds of elements on a metal substrate surface, the prediction of the growth mode or morphology is not straightforward, because of energetically complicated competition among two adsorbed elements and the substrate surface. However, for the systems with immiscible elements (denoted *A*, *B* for deposits, and *S* for the substrate), the growth mode becomes somewhat clear because of the existence of distinct interfaces. For example, three types of growth modes, (1) $A/B/S$, (2) $B/A/S$, and (3) $(A+B)/S$ with domains, are considered assuming *S* to be fixed as a substrate. The question, which type is the case, is a matter of the surface and interface energies, although the deposition sequence of *A* and *B* can be important under nonequilibrium conditions. The last type (3) is the present interest and, in this case, either deposit (*A* or *B*) will dominantly occupy the surface area depending on the sign of the energy difference, $\Delta\gamma=(\gamma_A+\gamma_{AS})-(\gamma_B+\gamma_{BS})$, e.g., for $\Delta\gamma<0$, *A* is dominant and, hereby, *B* may be piled up into 3D islands with small overall interface area on the substrate. In the above, γ_A and γ_B represent surface energies, and γ_{BS} and γ_{AS} interface energies.

This paper offers an example of morphological change caused by competition in surface and interface energies among immiscible constituents, leading to the nanostructuring of one of the constituents. We will show the dramatic morphological change of the preexisted Ag overlayer on the Ni(111) surface into 3D nanometer-scale islands (crystals) through the deposition of Pb onto the Ag/Ni(111) surface and, second, the formation of mobile nanoparticles by the deposition of Ag onto the Pb-covered Ni(111) surface. Also, we will describe the possibility of manipulating the nanostructuring.

II. EXPERIMENT

The experiments were carried out using a variable temperature scanning tunneling microscope (STM) set in an ultrahigh-vacuum chamber with facilities of an ion-sputtering gun, evaporation sources, and an equipment for surface chemical analysis. The substrate was a 4 N-pure Ni single crystal with the (111) face. The clean surface of the Ni(111) was prepared by repeated cycles of Ar^+ ion sputtering followed by successive annealing of the sample until atomically resolved STM images of the surface were obtained. The depositions of Ag and Pb were performed at rates of about 0.01 and 0.03 ML/min, respectively, at room temperature. Note that, in this paper, we define one monolayer (ML) as the amount of deposit corresponding to the completion of a monoatomic layer of Ag or Pb on the Ni(111) surface, not in the ordinary definition. The STM experiment was performed at room temperature in topographic mode

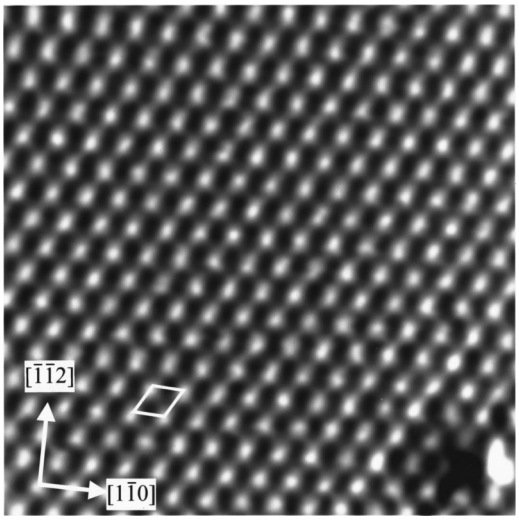

FIG. 1. STM image of the Ni(111) clean surface ($2.6 \times 2.6\ \mathrm{nm}^2$).

under a constant tunneling current. A typical image of the clean Ni(111) surface is shown in Fig. 1 with two crystal axes and the surface primitive unit mesh. The mesh side was measured to be 0.25 nm corresponding to the nearest-neighbor atomic distance in bulk Ni crystal.

III. RESULTS AND DISCUSSIONS

A. Deposition of Pb onto Ag/Ni(111)

As the first step, Ag was deposited on a Ni(111) surface at room temperature. At very low coverages, small 2D Ag islands grew out from descending Ni step edges. As the coverage increased, the islands extended, in 2D, to cover the whole terraces. Typical STM image ($150 \times 150\ \mathrm{nm}^2$) taken at a coverage of 0.5 ML is shown in Fig. 2(a), where Ag deposits are imaged as dendritic layer islands with broken edges each along the closed-packing direction ⟨110⟩. From several images at this stage, each island growth was found to be restricted within a single terrace domain. This means the existence of a potential barrier around the upper corner of the step, which depresses interlayer diffusions of Ag atoms. Upon further depositions, the Ag atoms filled the remaining area on the terrace up to a monolayer coverage. Figure 3 shows STM images obtained at about 1 ML of Ag. The deposited Ag layer exhibits a 7×7 moiré structure [Fig. 3(b)] with a period of about 1.8 nm (large dark spots) and the distinct sharp spots hexagonally arranged with the nearest-neighbor distance of about 0.3 nm. The nearest-neighbor distance for the sharp spots corresponds well to the value 0.29 nm of the bulk Ag. The lattice mismatch between Ag(111) and Ni(111) is about 16%. The large mismatch and the negligibly small solubility of Ag into Ni are consistent with the simple overlayer growth with the moiré structure. To our knowledge, the formation of a surface alloy has not yet been reported in the system Ag/Ni(111).[7,8] As described above, it is interesting to show how the morphology of the preexisting Ag layer was affected by the post-deposition of Pb, which has a much lower surface energy than Ag and Ni. Figure 4(a) shows the morphological change of the surface after the deposition of $\frac{2}{3}$ ML of Pb at room temperature. The preexisting 2D layer of Ag was drastically changed into 3D islands (highlighted portions), while deposited Pb atoms grow in 2D layer (dark region) covering the Ni(111) surface: The identification of the constituents was made by the detailed analysis (height analysis) of the cross section in STM images as described below. Let us assume the Ag islands are formed on the Ni(111) surface surrounded by the monoatomic Pb layer. From the height analysis in Fig. 4(b), the major part of

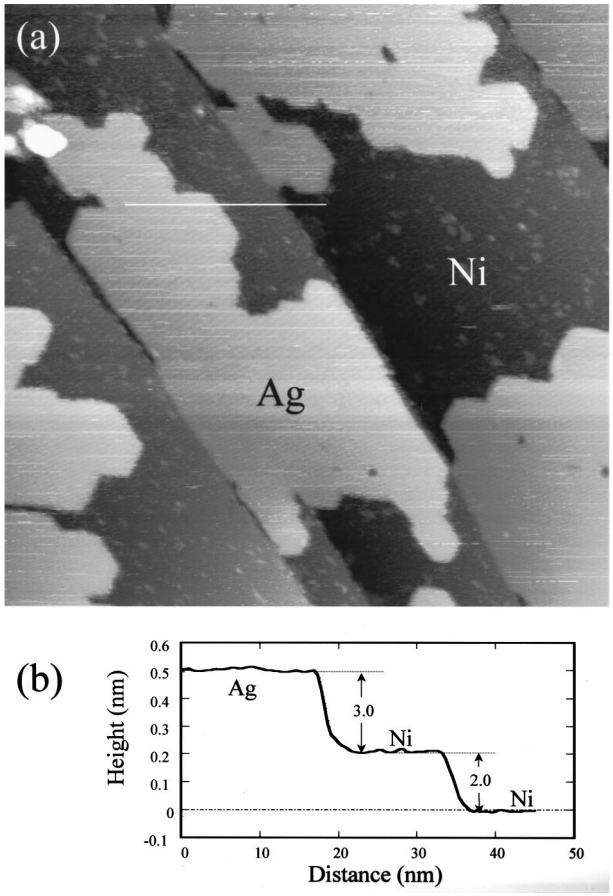

FIG. 2. (a) STM image of Ni(111) after deposition of 0.5 ML Ag ($150 \times 150\ \mathrm{nm}^2$) and (b) the line scan along the line marked by white segment in (a). Terminations of Ag islands at step edges are visible.

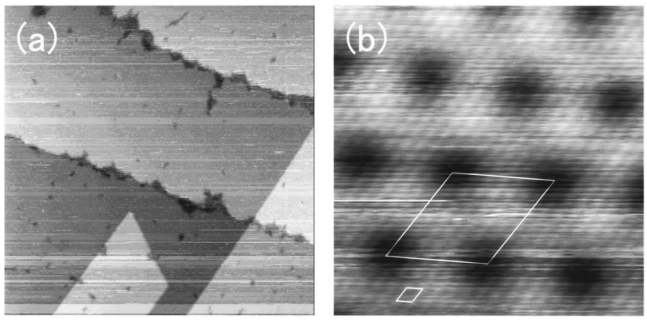

FIG. 3. (a) STM image at full monolayer coverage of Ag ($150 \times 150\ \mathrm{nm}^2$). (b) Atomically resolved image of the Ag layer ($68 \times 68\ \mathrm{nm}^2$): Large dark spots represent a long periodic interference pattern (moiré pattern) and distinct sharp spots (bright protrusions) correspond to the hexagonal close-packed layer of Ag(111) on Ni(111).

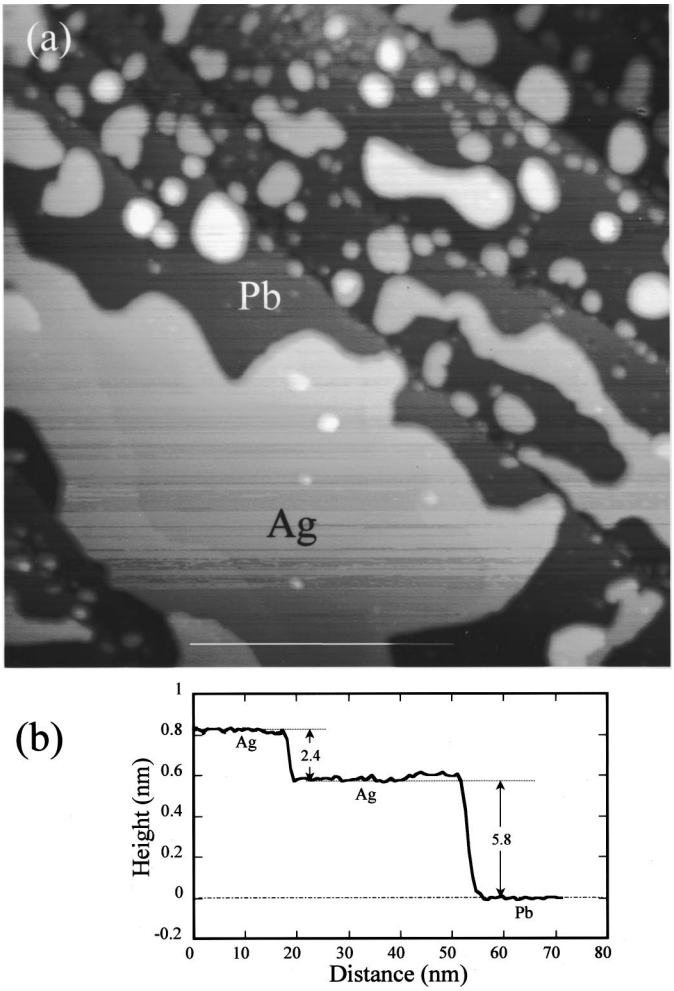

FIG. 4. (a) Morphological transition of the Ag 2D layer into 3D islands after Pb deposition of $\frac{2}{3}$ ML ($190\times190\,\mathrm{nm}^2$). (b) The line scan along the segment marked (white) in (a).

the Ag island is measured to 0.58 nm in height from the Pb layer. Considering the apparent height $d_{\mathrm{Pb\text{-}Ni}}=0.2$ nm of the Pb layer on Ni(111), which was measured in the following experiment on the Pb/Ni(111), the net height of the Ag island amounts to 0.78 nm with respect to the Ni(111) surface. This value just corresponds to the three monoatomic layers high of Ag(111) grown in contact with the Ni(111) surface, because the height includes $d_{\mathrm{Ag\text{-}Ni}}=0.3$ nm [see Fig. 2(b)], and two of $d_{\mathrm{Ag\text{-}Ag}}=0.24$ nm [see Fig. 4(b)]. The height differences observed at the present experiment are summarized in Fig. 5. The additional superstructure $\sqrt{3}$-Pb, partly formed on Ag islands, is of interest because of the incorporation of Pb

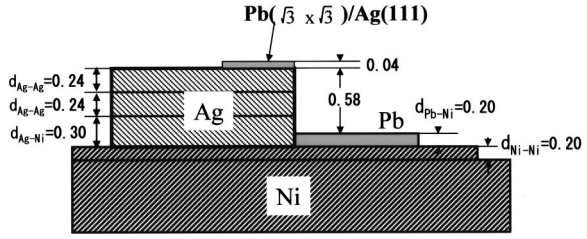

FIG. 5. Observed height differences from the STM image (Fig. 4): Heights for Pb and Ni (single atomic step) were measured using another STM image.

atoms into Ag(111) surface, but is not discussed more in this paper. The present analysis for the island formation is consistent with our previous work on the equivalent system by means of a low-energy ion-scattering spectroscopy,[9] where the monoatomic layer growth of Pb and the multilayered structure of Ag were clearly observed at the similar deposition and temperature. The formation of the three-monoatomic-layers-high islands, on average, leads to the decrease in effective coverage of Ag down to 33% of the substrate surface. The remaining area of 66% well corresponds to the area occupied by the $\frac{2}{3}$ ML Pb atoms deposited. The change of morphology from the 2D layer to 3D islands of Ag originates from the substitution of Pb atoms for the preexisting Ag atoms: The Pb atoms prefer to occupy the bare Ni(111) surface rather than on top of the Ag layer and this means the growth of the type (3) mentioned in the Introduction. The observed height, 0.3 nm, for the Ag layer just above the substrate [see Fig. 2(b)] is considerably larger than the Ag-Ag interlayer spacing, 0.24 nm, but rather close to the atomic diameter of Ag (0.29 nm): This is explained mainly by an increase in average height resulting from the lattice mismatch between Ag(111) and Ni(111). On the contrary, the apparent height (0.2 nm) of Pb layer is much less than the atomic diameter (0.35 nm) of Pb atom and therefore, cannot be interpreted in terms of the lattice mismatch between Pb(111) and Ni(111); probably coming from the difference in electronic states on the surfaces between Pb/Ni(111) and Ni(111).

The STM image in Fig. 6(a) corresponds to the Pb coverage of about 1 ML at room temperature. In this figure, the morphology is further changed into discrete dots of nanosize crystals of Ag (bright dots) with hexagonal shaped edges [see high-quality image inseted in Fig. 6(a)]. The major part of the image (dark region) is covered by a monoatomic Pb layer, although, in some places, small 3D islands of Pb [indicated by white arrow in Fig. 6(a)] exist because of the presence of excess Pb atoms not substitutable for Ag atoms. The size distribution of the Ag nanocrystals is plotted in Fig. 6(c), where the data were accumulated from several images showing similar features to Fig. 6(a). The average size of the crystals was estimated to about 7 nm in diameter. The height of the Ag crystals is estimated to about 2.5 nm on average (about 10 monoatomic layers high). This indicates the decrease of the effective Ag coverage down to about 0.1 ML (10%) of the substrate surface. The coverage can be compared with the observed bright area (13%) of the image. According to a simple thermodynamic consideration, the increase of the island height results in the decrease of surface energy of the system due to the increase of the portion occupied by the low-surface energy Pb. However, not many high islands were observed in the present experiment (the aspect ratio was about $\frac{1}{3}$). Two reasons are considered: one is the limited mobility or diffusion length of Ag or Pb atoms at room temperature, and the second is the increase in the surface energy resulting from the increased area of the side walls of Ag crystals. Figure 7 illustrates a model of the Ag nanocrystal formed on Ni(111) surface with the monoatomic Pb layer. The side walls of the Ag crystal are assumed to have possible close-packed faces, the {111} and {100} planes, to achieve minimum surface energy and to also reproduce the observed hexagonal shaped edges of the crystals [see

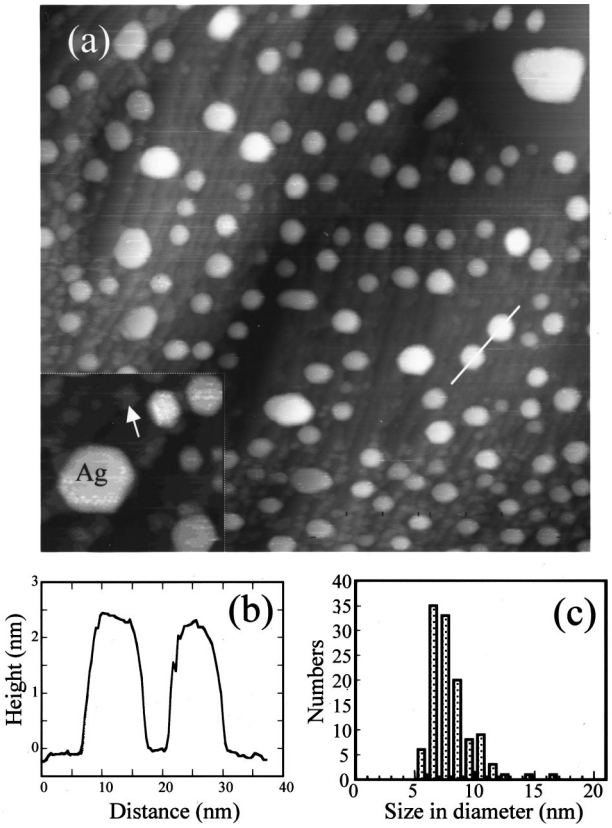

FIG. 6. (a) Nanostructuring of Ag atoms observed at 1 ML Pb deposition; bright dots, Ag nano-crystals; dark region, Pb monoatomic layer ($230\times230\,\mathrm{nm}^2$). A high-quality image of the islands with hexagonal shaped edges are inseted in the lower part of this figure ($50\times50\,\mathrm{nm}^2$). (b) The line scan along the segment marked (white) in (a). (c) Size distribution of Ag nanocrystals.

high-quality image in Fig. 6(a)]. The characteristic feature of the Ag nanocrystals obtained in the present experiment is that they are directly coupled with the Ni(111) surface, not on the Pb layer but surrounded by the Pb layer as described above. This can be compared with the following result.

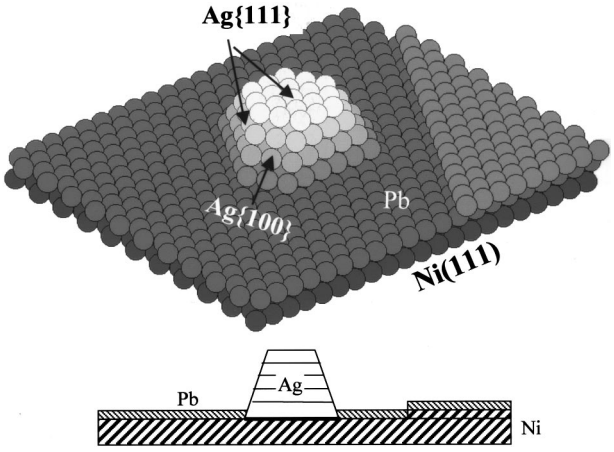

FIG. 7. A model of Ag nanocrystal. The crystal walls were assumed to have low surface energy planes, the {111} and {100}. For simplicity, lattice mismatches are not taken into account.

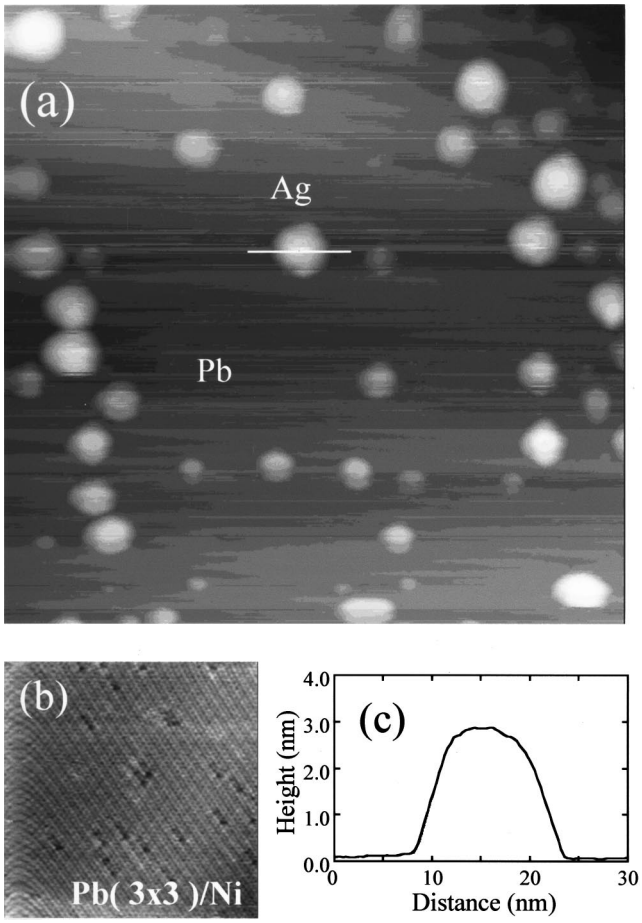

FIG. 8. (a) Nanoparticles formed on the Pb layer after 0.2 ML Ag deposition onto the Pb-covered Ni(111) surface ($190\times190\,\mathrm{nm}^2$). (b) A moiré structure ($\sim3\times3$) at 1 ML Pb deposition on Ni(111) ($20\times20\,\mathrm{nm}^2$). (c) The line scan along the segment marked (white) in (a).

B. Deposition of Ag onto Pb/Ni(111)

In the previous section, we described the dramatic change in surface morphology from 2D overlayer to 3D nanocrystals of Ag during Pb deposition onto the Ag/Ni(111) surface. The driving force for the nanostructuring comes from the energy gain by substituting adsorbed Pb atoms for preexisting Ag atoms. One may ask, because surface morphologies are frequently determined by a kinetic process of adsorption rather than by thermodynamic equilibrium what differences would be expected to appear between the case of Ag deposition on Pb/Ni(111) and that of Pb on Ag/Ni(111). Accordingly, in this section, we examine the growth morphologies of Ag deposited onto a Pb precovered Ni(111) surface.

We demonstrate in Fig. 8(a), a typical image of the surface morphology at 0.2 ML deposition of Ag at room temperature after the deposition of 1 ML Pb on Ni(111), where Pb layer exhibits 3×3 superstructure [Fig. 8(b)], similar to the case of Pb/Cu(111),[10,11] depending on the coverage.[12] Again, the formation of Ag nanoparticles was observed; namely the Volmer-Weber growth mode proceeded. Here, the description ''nanoparticles'' not ''nanocrystals'' was employed because we have no information about the crystal structure of the particles at present. The relation $\gamma_{\mathrm{Ag}}+\gamma_i-\gamma_{\mathrm{Pb}}>0$ required for the Volmer-Weber growth mode is

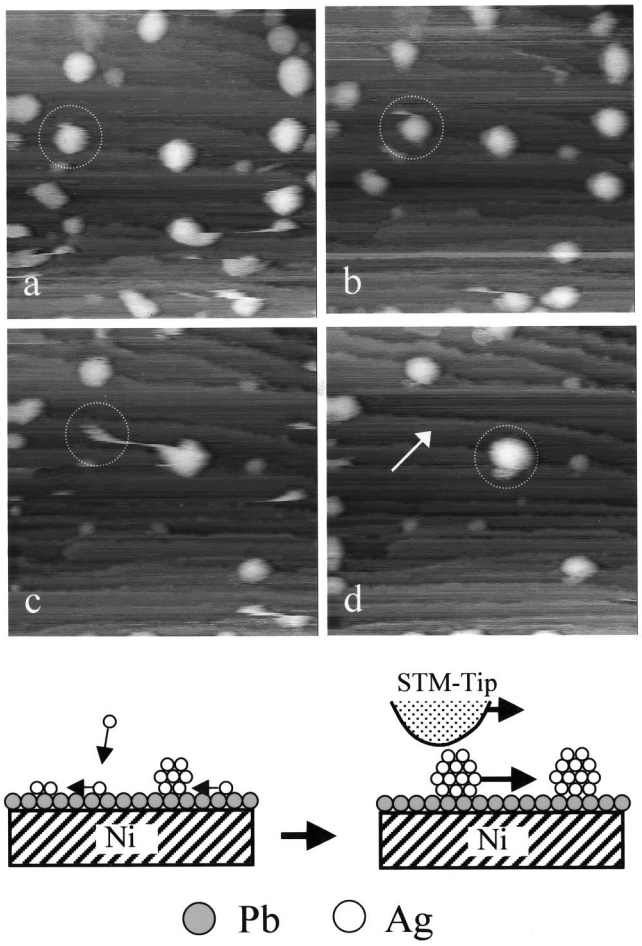

FIG. 9. Four consecutive STM scans taken after deposition of 0.2 ML Ag onto Pb-covered Ni(111) surface ($115\times115\,\mathrm{nm}^2$: $Vs=-0.51$ V, $I=0.2$ nA). It should be noted that there are no traces of vacant holes of Pb after the movements of the Ag particle marked by the dotted circle.

evident, because $\gamma_{\mathrm{Ag}}>\gamma_{\mathrm{Pb}}$ for surface energies and $\gamma_i>0$ (from the positive heat of formation of Pb-Ag alloy) for interface energy are not in doubt. There are, however, important differences between the case described above and the present one. To see this, we depicted four consecutive scans of STM images in Figs. 9(a)–9(d). In these figures, we can see drastic movements of nanoparticles dragged by tip motions; some particles are moved from one place to another, and others outside the image [compare the number of particles appearing in Figs. 9(a) and 9(d)]; the particle marked by dotted circles just incorporates with another after traveling about 40 nm along the step. It is noticed that there are no visible traces of vacant holes of Pb at the original position of the particle (marked by the white arrow). This implies that Ag particles are formed on the preexisting Pb monoatomic thin layer without any substitutions for Pb, never on the bare Ni(111) surface. The easy movement of Ag particles by tip motions is, thus, explained in terms of weak interactions at interfaces between the Ag particles and Pb layer. On the other hand, no movements have been observed in the previous case of Pb deposition on Ag/Ni(111). This is because Ag nanocrystals are directly coupled with the Ni(111) surface, and further, firmly locked by the surrounding monoatomic Pb.

Finally, there are many possible candidates for the combination of deposited and substrate elements [e.g., (Bi, Ag)/Pt; (Pb, Cu)/W; etc.], on which one of the deposited elements is expected to exhibit nanostructuring behavior on the substrate surface similar to the present cases. If we properly design the system, including the step alignment on the substrate surface, and control the deposition sequence, it may be possible to create new functional nanostructured material, including nanoalloying, because we have two types of nanoparticles: one is tightly fixed to the substrate (utilized as a fixed point), and the other is mobile (utilized for geometrical positioning and alloying, if necessary).

IV. SUMMARY

We have investigated the nanostructuring process of Ag atoms on the Ni(111) surface in two different ways: (1) the use of a morphological change resulting from the Pb deposition onto the Ag-covered Ni(111) surface, and (2) the use of Volmer-Weber growth mode by Ag deposition onto Pb-covered Ni(111) surface. In case (1), we observed the morphological change of Ag atoms from 2D layer to 3D islands in the course of Pb deposition at room temperature, due to substitutions of deposited Pb atoms for preexisting Ag atoms, leading to the formation of Ag nanocrystals at about a full monolayer coverage of Pb. The nanocrystals are tightly bounded to the substrate surface because they are directly coupled with the Ni(111) surface and surrounded by the monoatomic Pb layer. In case (2), deposited Ag atoms were condensed into nanoparticles without any substitution of Ag for Pb atoms, where the Ag particles are formed immediately on top of the preexisting Pb layer, not on the Ni surface. The particles were found to be mobile under the interaction with scanning STM tip. The nanostructuring of Ag was explained by kinetic processes and simple thermodynamic considerations. Also, the possibility to design nanostructures, including nanoalloy formation, was described.

[1] Zhenyu Zhang and Max G. Lagally, Phys. Rev. Lett. **72**, 693 (1994).
[2] J. Vrijmoeth, H. A. van der Vegt, J. A. Meyer, E. Vlieg, and R. J. Behm, Phys. Rev. Lett. **72**, 3843 (1994).
[3] M. A. Boshart, A. A. Bailes III, and L. E. Seiberling, Phys. Rev. Lett. **77**, 1087 (1996).
[4] M. Breeman, G. T. Barkema, M. H. Langelaar, and D. O. Boerma, Thin Solid Films **272**, 195 (1996).
[5] I. S. Hwang, T. C. Chang, and T. T. Tsong, Surf. Sci. Lett. **410**, L741 (1998).
[6] E. Bauer, Z. Kristallogr. **110**, 372 (1958).
[7] F. Besenbacher, L. P. Nielsen, and P. T. Sprunger, in *The Chemical Physics of Solid Surfaces*, edited by D. A. King and D. P. Woodruff (Elsevier, Amsterdam, 1997), Vol. 8, p. 237.
[8] T. Itoh, K. Umezawa, and S. Nakanishi, Appl. Surf. Sci. **130-132**, 497 (1998).

[9] T. Itoh, S. Nakanishi, K. Umezawa, S. Yamamoto, K. Narumi, and H. Naramoto, JARE TIARA Report No. 99, 1999 (unpublished), p. 182.
[10] C. Nagl, M. Schmid, and P. Varga, Surf. Sci. **369**, 159 (1996).
[11] G. Meyer, M. Michailov, and M. Henzler, Surf. Sci. **202**, 125 (1988).
[12] K. Umezawa, A. Takahashi, T. Yumura, S. Nakanishi, and W. M. Gibson, Surf. Sci. **365**, 118 (1996).